

Inertial and gravity wave transmissions near the radiative-convective boundaries

Tao Cai¹†, Cong Yu^{2,1}‡ and Xing Wei³

¹State Key Laboratory of Lunar and Planetary Sciences, Macau University of Science and Technology, Macau, People's Republic of China

²School of Physics and Astronomy, Sun Yat-sen University, Zhuhai, 519082, People's Republic of China

³Department of Astronomy, Beijing Normal University, Beijing, People's Republic of China

(Received xx; revised xx; accepted xx)

In this paper, we study the inertial and gravity wave transmissions near the radiative-convective boundaries in the f -plane. Two configurations have been considered: waves propagate from the convective layer to the radiative stratified stable layer, or the other way around. It has been found that waves prefer to survive at low latitudes in a slowly rotating fluid (the stable layer is strongly stratified). When the rotation is rapid (the stable layer is weakly stratified), however, waves can survive in the full sphere if the meridional wavenumber is large. Then we have discussed the transmission ratios for two different stratified structures: the constant stratification, and the continuously varying stratification. For the constant stratification, we have found that the transmission is efficient when the rotation is rapid, or when the wave is near the critical colatitude. For the continuously varying stratification, we have discussed the transmission ratio when the square of buoyancy frequency is a polynomial function $N^2 \propto z^\nu$. For the linear stratification ($\nu = 1$), we have found that the transmission is efficient when the rotation is rapid, or when the wave is near the critical colatitude, or when the width of the linear stratification layer is far greater than the horizontal wave length. For a convex stratification ($\nu > 1$), the incident wave is always transmitted. For a concave stratification ($0 < \nu < 1$), the incident wave is always reflected. The transmission ratios does not depend on the configurations, but only on the characteristics of the wave (frequency and wavenumber) and the fluid (degree of stratification).

Key words:

1. Introduction

Wave propagation is an important physical process in stars and planets. For example, it is well known that internal gravity waves (IGWs) are likely to be generated near the radiative-convective boundary in stars by the shear stress (Kumar *et al.* 1999) or the stochastic overshooting plumes (Rogers & Glatzmaier 2005; Mathis *et al.* 2014). When IGWs propagate in the radiative stable layer, it could induce material mixing (Rogers & McElwaine 2017) and transport angular momentum (Rogers *et al.* 2013; Fuller *et al.* 2014). For a stable layer above a convective layer, gravity wave is important because

† Email address for correspondence: tcai@must.edu.mo

‡ Email address for correspondence: yucong@mail.sysu.edu.cn

gravity waves propagate upward into a decreasing density region, which yields increasing wave amplitudes and wave breaking (Rogers *et al.* 2013). On Earth's atmosphere, it has been confirmed that the breaking of gravity wave is one of the major factors for the transport of water from troposphere into the stratosphere (Qu *et al.* 2020). Using the analogy of Earth's atmosphere, Rogers *et al.* (2013) proposed that IGW is dynamically and chemically important in massive stars. Recently, low-frequency gravity waves were indeed detected in blue supergiants by the method of asteroseismology (Bowman *et al.* 2019). Wave propagation also plays an essential role on angular momentum transport. Zahn *et al.* (1997) developed a theoretical model on the angular momentum transported by waves. For stars, the model of Fuller *et al.* (2014) predicts that IGW tends to reduce differential rotation on short timescales in low mass stars. Thus it helps to explain the observed small amounts of internal differential rotation in the low-mass main-sequence stars. For planets, Rogers *et al.* (2012) have shown that the misalignment of exoplanets around hot stars can be naturally explained by the angular momentum transport driven by IGWs. In short-period exoplanets, the thermal tides from the host star can also generate IGWs. Analysis of IGWs in short-period exoplanets revealed that the angular momentum transport could be enhanced when the radiative-convective boundary is in the vicinity of the thermal forcing penetration depth (Yu 2020). Apart from gravity waves, inertial waves could also be generated in rotating stars or planets (Ogilvie & Lin 2004; Wu 2005a; Goodman & Lackner 2009). Estimation of tidal quality factor illustrated that the resonantly excited inertial modes have significant impact on the tidal dissipation of a coreless Jupiter (Wu 2005b). Goodman & Lackner (2009) argued that a rigid core should be included in the model, and tidal calculations by Wu (2005b) might underestimate the tidal quality factor. In the discussion of Goodman & Lackner (2009), the inertial waves were assumed to be fully reflected at the surface of the rigid core. However, recent study (Liu *et al.* 2019) revealed that Jupiter probably has a diluted core formed by a giant impact. If the rigid core is replaced by a diluted core, the inertial waves are expected to be partially reflected at the surface. An analogy can be readily drawn between this problem and that of wave propagations near the radiative-convective boundaries.

A question that remains unclear is how the waves reflect and transmit near the radiative-convective boundaries in stars and planets. Wei (2020) has discussed the reflection and transmission of an incident wave at the radiative-convective boundary in the f -plane, with the assumption that the buoyancy frequency abruptly changes from zero at the convective layer to a constant value at the radiative stable layer. He discovered that waves can efficiently transmit across the boundary in the rapidly rotating fluid. In real stars or planets, the transitions of thermal structures are likely to be continuous. Therefore it is necessary to consider the wave reflection and transmission near a continuously transited radiative-convective boundary. In this paper, we extend the work of Wei (2020), by considering two different stratification structures in the stable layer: the constant stratification, and the continuously varying stratification. Efficiencies of wave transmissions were estimated and compared.

2. Method and result

For a Boussinesq flow in a rotating f -plane, the linearized hydrodynamic equations of mass and momentum conservations are

$$\nabla \cdot \mathbf{u} = 0 , \quad (2.1)$$

$$\mathbf{u}_t + \mathbf{f} \times \mathbf{u} + \nabla p - b\hat{\mathbf{z}} = 0 , \quad (2.2)$$

$$b_t + N^2 \mathbf{u} \cdot \hat{\mathbf{z}} = 0 . \quad (2.3)$$

where $\mathbf{u} = (u, v, w)$ is the velocity; $\mathbf{f} = (0, \tilde{f}, f)$ is a vector form of horizontal and vertical Coriolis parameters, with $\tilde{f} = 2\Omega \sin \theta$ and $f = 2\Omega \cos \theta$; Ω is the rotation rate, and θ is the colatitude of the f -plane; p is the modified pressure perturbation (pressure perturbation scaled by constant background density); b is the buoyancy; g is the gravity; N^2 is the square of buoyancy frequency; $\hat{\mathbf{x}}$, $\hat{\mathbf{y}}$, and $\hat{\mathbf{z}}$ are the unit vectors in the east-west direction, the south-north direction, and the vertical direction, respectively. We consider a two-layer thermal structure, with an upper density-stratified stable layer adjacent to a lower adiabatically convective layer (fig.1a). By this setting, N^2 is positive in the stable layer, and zero in the convective layer, respectively. After some manipulations, the above equations can be reduced into the following equation on vertical velocity (Gerkema & Shrira 2005):

$$\nabla^2 w_{tt} + (\mathbf{f} \cdot \nabla)^2 w + N^2 \nabla_h^2 w = 0 , \quad (2.4)$$

where $\nabla_h^2 = \partial_x^2 + \partial_y^2$ is the horizontal Laplacian operator, and $\nabla^2 = \nabla_h^2 + \partial_z^2$ is the Laplacian operator. For a plane wave propagating in the direction $(\cos \alpha, \sin \alpha)$, the problem can be further simplified by introducing a new variable χ , which satisfies $x = \chi \cos \alpha$ and $y = \chi \sin \alpha$ (fig.1b). Substituting $\partial_x = \cos \alpha \partial_\chi$, $\partial_y = \sin \alpha \partial_\chi$, and $w = W(\chi, z) \exp(-i\sigma t)$ into the above equation, we obtain

$$AW_{\chi\chi} + 2BW_{\chi z} + CW_{zz} = 0 , \quad (2.5)$$

where σ is the time frequency, $A = \tilde{f}_s^2 - \sigma^2 + N^2$, $B = f\tilde{f}_s$, $C = f^2 - \sigma^2$, and $\tilde{f}_s = \tilde{f} \sin \alpha$. Wave solution exists when this partial differential equation is hyperbolic, thus it requires $\Delta = B^2 - AC > 0$ (Gerkema & Shrira 2005), or equivalently

$$\sigma^4 - (f^2 + \tilde{f}_s^2 + N^2)\sigma^2 + N^2 f^2 < 0 . \quad (2.6)$$

Then the frequency range for wave solutions is

$$\sigma_1^2 < \sigma^2 < \sigma_2^2 , \quad (2.7)$$

where $\sigma_{1,2}^2 = [(f^2 + \tilde{f}_s^2 + N^2) \mp \sqrt{(f^2 + \tilde{f}_s^2 + N^2)^2 - 4N^2 f^2}]/2$. For a wave to propagate through the whole domain, this inequality should be satisfied for all the possible values of $N^2(z)$. Let N_{min}^2 and N_{max}^2 be the minimum and maximum values of $N^2(z)$, respectively. For a wave to survive in both convective and stable layers, it requires

$$\sigma_{min}^2 < \sigma^2 < \sigma_{max}^2 , \quad (2.8)$$

where $\sigma_{min}^2 = [(f^2 + \tilde{f}_s^2 + N_{max}^2) - \sqrt{(f^2 + \tilde{f}_s^2 + N_{max}^2)^2 - 4N_{max}^2 f^2}]/2$ and $\sigma_{max}^2 = [(f^2 + \tilde{f}_s^2 + N_{min}^2) + \sqrt{(f^2 + \tilde{f}_s^2 + N_{min}^2)^2 - 4N_{min}^2 f^2}]/2$. In our problem $N_{min}^2 = 0$, thus $\sigma_{max}^2 = f^2 + \tilde{f}_s^2$. The width of the frequency range is

$$\sigma_{max}^2 - \sigma_{min}^2 = \frac{1}{2}[(f^2 + \tilde{f}_s^2 - N_{max}^2) + \sqrt{(f^2 + \tilde{f}_s^2 + N_{max}^2)^2 - 4N_{max}^2 f^2}] \quad (2.9)$$

$$= \frac{1}{2}[(f^2 + \tilde{f}_s^2 - N_{max}^2) + \sqrt{(f^2 + \tilde{f}_s^2 - N_{max}^2)^2 + 4N_{max}^2 \tilde{f}_s^2}] . \quad (2.10)$$

This width is always positive unless $\tilde{f}_s^2 = 0$ and $f^2 + \tilde{f}_s^2 \leq N_{max}^2$. $\tilde{f}_s^2 = 0$ can be achieved only when $\sin \theta = 0$ or $\sin \alpha = 0$. Thus, in polar regions, waves cannot survive in both convective and stable layers in a slowly rotating fluid ($N^2/4\Omega^2 \gg 1$, or in other words, the stable layer is strongly stratified) (Wei 2020). However, the conclusion at other latitudes is completely different. At other latitudes, if the meridional wavenumber is nonzero, waves can survive in both convective and stable layers even in a slowly rotating fluid.

The width of the frequency range decreases with $N_{max}^2/4\Omega^2$ (see Appendix A), with an upper limit value $f^2 + \tilde{f}_s^2$ achieved at $N_{max}^2/4\Omega^2 \rightarrow 0$ and a lower limit value \tilde{f}_s^2 achieved at $N_{max}^2/4\Omega^2 \rightarrow \infty$. As a result, waves are more likely to survive at low latitudes in a slowly rotating fluid, where \tilde{f}_s^2 is larger. In a rapidly rotating fluid ($N^2/4\Omega^2 \ll 1$, or in other words, the stable layer is weakly stratified), waves are more likely to survive at high latitudes, but the chance at low latitudes is still moderate if the meridional wavenumber dominates the zonal wavenumber. If N_{max}^2 is fixed, it is obvious that the width increases with $\sin^2 \alpha$ (see Appendix A). Thus waves with higher meridional wavenumbers are more likely to survive. The dependence of width on θ can be analyzed by taking the first derivative of θ . For the simplicity of explanation, we only consider the northern atmosphere. The case in the southern atmosphere can be inferred from the symmetric property. After some trivial calculation (see Appendix A), we find that the conclusion depends on $N_{max}^2/4\Omega^2$ and $\sin^2 \alpha$. If $N_{max}^2/4\Omega^2 > 1$, then the width increases with θ . If $N_{max}^2/4\Omega^2 < 1$, there exists a critical value $(\sin^2 \alpha)_c$. The width increases with θ in the range $\sin^2 \alpha > (\sin^2 \alpha)_c$, and decreases with θ in the range $\sin^2 \alpha < (\sin^2 \alpha)_c$. Again, we have verified that the frequency range is wider at low latitudes in a slowly rotating fluid. In a rapidly rotating fluid, waves can survive in the full sphere when the meridional wavenumber is large (see fig. 5(a) in Appendix A).

Given σ in the frequency range $(\sigma_{min}, \sigma_{max})$, the wave solution can be obtained if $W(\chi, z)$ is solvable. The general solution of (2.5) can be written in a form (Gerkema & Shrira 2005) of

$$W = \Psi(z) \exp(ik\chi) = \psi(z) \exp i(k\chi + \delta z), \quad (2.11)$$

where $\delta = -kB/C$ and $\Psi(z) = \psi(z) \exp(i\delta z)$. Making a substitution, we obtain

$$\psi_{zz} + k^2 \left(\frac{B^2 - AC}{C^2} \right) \psi = 0. \quad (2.12)$$

or

$$\psi_{zz} + \frac{k^2}{C} \left(\frac{B^2 - A_0 C}{C} - N^2 \right) \psi = 0, \quad (2.13)$$

where $A_0 = \tilde{f}_s^2 - \sigma^2$. From this equation, we know that the wave solution depends on the structure of $N^2(z)$.

Before the discussion of wave transmission, it is necessary to consider the wave directions in detail. Here we determine the wave direction by its group velocity, because it represents the direction of energy propagation. For the convenience of discussion, let us first consider a simple case with constant N^2 . In such case, the basis functions of wave solution can be written as $e^{i(\pm r_0 + \delta)z}$, where $r = \pm r_0 + \delta$ is the wavenumber along the vertical direction. For the convenience of discussion, we call $\pm r_0$ as modified vertical wavenumber. Substituting $e^{\pm i r_0 z}$ into (2.12), we obtain the dispersion relation

$$r_0^2 = k^2 \frac{B^2 - AC}{C^2}. \quad (2.14)$$

Taking the first derivative to σ , we have

$$\frac{dr_0}{d\sigma} = \frac{k^2 \sigma}{r_0} \frac{C^2 - AC + 2B^2}{C^3}, \quad (2.15)$$

where $c_{g0} = d\sigma/dr_0$ is the modified vertical group velocity, and $c_{p0} = \sigma/r_0$ is the modified vertical phase velocity. Let us define a quadratic function $h(C) = C^2 - AC + 2B^2$. It can be easily proved that $h(C) = C^2 + B^2 + (B^2 - AC) > 0$ if wave solution exists.

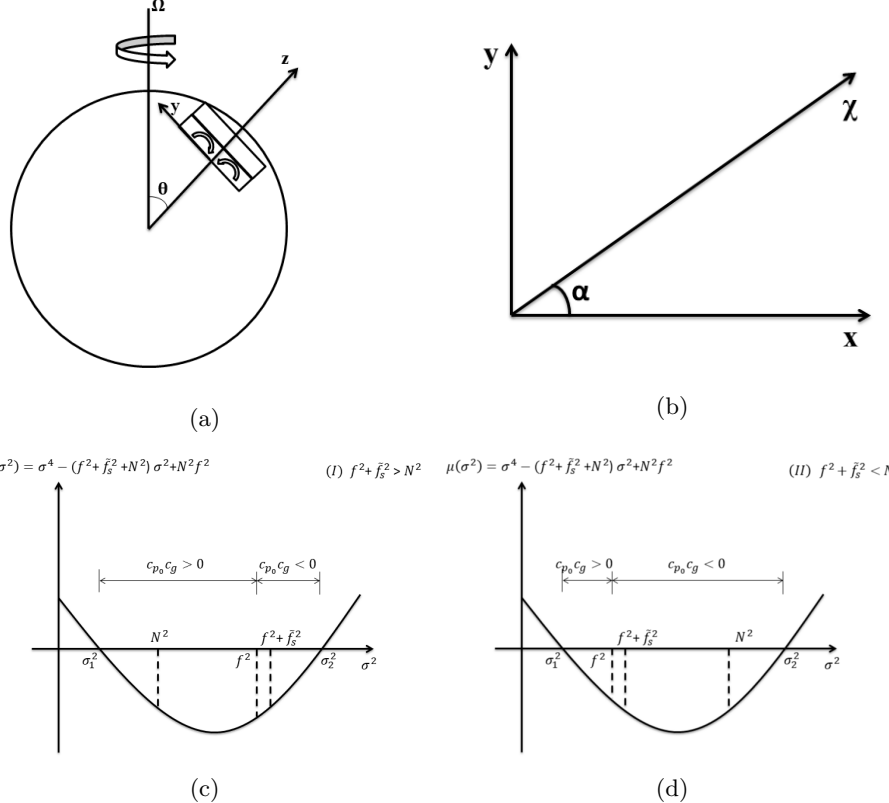


Figure 1: Sketch plots of f -plane structure and wave direction. (a) Illustration of a two-layer setting f -plane. The stable layer sits above the convective layer. The f -plane is inclined an angle θ with the north pole. \hat{y} is the south-north direction. \hat{z} is the vertical direction. \hat{x} is the east-west direction pointing into the plane of the paper. (b) The plane wave propagates in a direction at an angle α to x -axis. (c) and (d) The sign of $c_{p0}c_g$ in weakly (case I) and strongly (case II) stratified cases, respectively. Note that f^2 can be smaller than N^2 in the weakly stratified case.

Now we consider the vertical group velocity of the wave e^{irz} . It can be shown that

$$\begin{aligned} \frac{dr}{d\sigma} &= \pm \frac{dr_0}{d\sigma} + \frac{d\delta}{d\sigma} \\ &= \frac{k\sigma}{C^2} \left[\frac{\pm(C^2 - AC + 2B^2) - 2B(B^2 - AC)^{1/2}}{(B^2 - AC)^{1/2}} \right], \end{aligned} \quad (2.16)$$

where $c_g = d\sigma/dr$ is the vertical group velocity, and c_p is the vertical phase velocity. Note that c_g has the same sign as $dr/d\sigma$. Compared to group velocity, the judgement of phase velocity direction is much easier. So here we try to build up some relations between the vertical group velocity c_g and the modified phase velocity c_{p0} . It can be shown that

$$\begin{aligned} \frac{r_0}{\sigma} \frac{dr}{d\sigma} &= \frac{kr_0}{C^2} \left[\frac{\pm(C^2 - AC + 2B^2) - 2B(B^2 - AC)^{1/2}}{(B^2 - AC)^{1/2}} \right] \\ &= \frac{k^2}{C^3} \left[\frac{\pm(C^2 - AC + 2B^2) - 2B(B^2 - AC)^{1/2}}{(B^2 - AC)^{1/2}} \right] \left[\pm(B^2 - AC)^{1/2} \right] \end{aligned}$$

$$= \frac{k^2}{C^3} [(C^2 - AC + 2B^2) \mp 2B(B^2 - AC)^{1/2}] . \quad (2.17)$$

It is easy to prove $h(C) > |2B(B^2 - AC)^{1/2}|$ since

$$(C^2 - AC + 2B^2)^2 - 4B^2(B^2 - AC) = (C^2 - AC)^2 + 4B^2C^2 > 0 . \quad (2.18)$$

Thus we conclude that

$$Sgn(c_g c_{p_0}) = Sgn\left(\frac{r_0}{\sigma} \frac{dr}{d\sigma}\right) = Sgn(C) , \quad (2.19)$$

where the operator Sgn is a sign function. As a result, the sign of $c_{p_0} c_g$ is only determined by the sign of C . When $\sigma^2 < f^2$, c_g and c_{p_0} are in the same direction. When $\sigma^2 > f^2$, c_g is in the opposite direction with c_{p_0} . Singularity appears when $\sigma^2 = f^2$ and it defines the critical colatitudes $\theta_c = \cos^{-1} \pm \sigma/(2\Omega)$ (Rieutord *et al.* 2001; Goodman & Lackner 2009). Our conclusion is general for the wave propagation in a tilted f -plane. The special cases of the pure gravity wave ($f^2 = 0$) and the pure inertial wave ($N^2 = 0$) have been well studied in a non-tilted plane ($\tilde{f}^2 = 0$ and $c_{p_0} = c_p$) (Rieutord 2015). For the pure gravity wave case ($f^2 = 0$ and $\tilde{f}^2 = 0$), we have $f^2 = 0 < \sigma^2 < N^2$. Thus c_g always propagates in the opposite direction to c_p . For the pure inertial wave case ($N^2 = 0$ and $\tilde{f}^2 = 0$), we have $0 < \sigma^2 < f^2$. Thus c_g always propagates in the same direction as c_p . These two results are implied in the calculations of Rieutord (2015) (see equations (5.48) and (8.20) in the book). Now let us consider the gravito-inertia wave in the non-tilted f -plane ($f = 0$ and $\tilde{f} = 2\Omega$). For such case, the lower and upper limits of wave frequency are $\sigma_{1,2}^2 = (f^2 + N^2 \mp |f^2 - N^2|)/2$. When the density structure is weakly stratified $N^2/f^2 < 1$, we have $\sigma^2 < \sigma_2^2 = f^2$, therefore c_g has the same direction as c_p . When the density structure is strongly stratified $N^2/f^2 > 1$, we have $f^2 = \sigma_1^2 < \sigma^2$, therefore c_g has the opposite direction to c_p . When $N^2/f^2 = 1$, $c_g = 0$ and wave energy does not propagate along the vertical direction. Clearly, the direction of c_g depends on the density stratification. In summary, c_g in weakly (strongly) stratified density structure prefers the same (opposite) direction as (to) c_p . Now we consider the more general case for the gravito-inertia wave in a tilted f -plane ($\tilde{f} \neq 0$). The discussion is similar to that of the non-tilted case. If $\tilde{f}_s \neq 0$, then $\sigma^2 \in (\sigma_1^2, \sigma_2^2)$ can be separated into two regions. In the region $\sigma_1^2 \in (\sigma_1^2, f^2)$, c_g has the same direction as c_{p_0} (fig. 1(c)). On the other hand, in the region $\sigma^2 \in (f^2, \sigma_2^2)$, c_g has the opposite direction to c_{p_0} (fig. 1(d)). In the strongly stratified (slowly rotating) case, the frequency range of $c_{p_0} c_g > 0$ is thinner than that of $c_{p_0} c_g < 0$. So c_g and c_{p_0} prefers the opposite direction in a strongly stratified density structure. In a weakly stratified (rapidly rotating) case, the conclusion depends on latitudes. They prefers the same direction at high latitudes, but the opposite direction at low latitudes.

Now we discuss the wave reflection and transmission at the interface between the convective layer and the density-stratified stable layer. Wei (2020) has discussed four configurations on wave reflection and transmission: from convective (stable) to stable (convective) layers, and stable layer sitting above (below) convective layer. It is easy to verify that when the stable layer is switched with the convective layer, the Boussinesq equations in the f -plane are invariant under the transformation $z \leftrightarrow -z$ and $w \leftrightarrow -w$, where the location of the interface is set at $z = 0$. Thus it is sufficient to discuss one of the cases. The other case can be inferred from the symmetric property. In this paper, we consider two configurations for the stable layer sitting above the convective layer: the wave propagates from the convective layer to stable layer (the left panel of fig. 2), and the wave propagates from the stable layer to the convective layer (the right panel of fig. 2). In either case, we consider two different stratification structures in the stable layer:

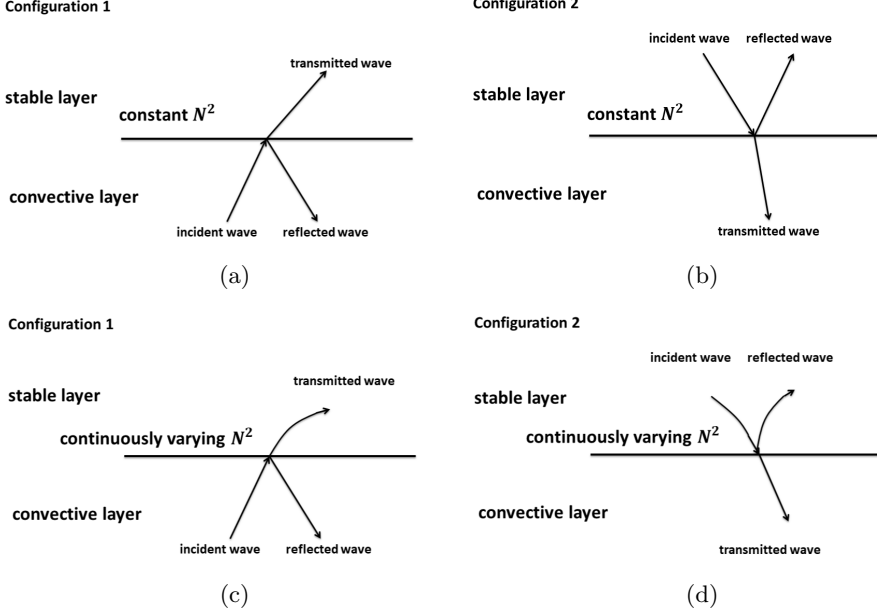


Figure 2: Sketch plots of wave propagation in different configurations. (a and c) Configuration 1: the wave propagates from the convective layer to the stable layer. (b and d) Configuration 2: the wave propagates from the stable layer to the convective layer. (a and b) The stable layer is constant stratification. (c and d) The stable layer is continuously varying stratification.

constant stratification (fig. 2(a and b)), and continuously varying stratification (fig 2(c and d)).

To obtain the wave solution, we firstly discuss the general solutions in the convective layer and the stable layer, and then determine the coefficients by matching boundary conditions at the interface. We have two boundary conditions at the interface. The first is the condition for continuous vertical velocity $w(0^+) = w(0^-)$. The second is the condition that Lagrangian perturbation of pressure is continuous at the interface, which requires that the first derivative of vertical velocity is continuous $w_z(0^+) = w_z(0^-)$ (see Wei (2020) and Appendix B for explanation).

In the adiabatically convective layer with $N^2 = 0$, it is easy to obtain the following wave solution:

$$\psi = a_1 \exp(iqz) + a_2 \exp(-iqz) , \quad (2.20)$$

where $q > 0$ and $q^2 = k^2(B^2 - A_0C)/C^2$ is the square of wavenumber in the vertical direction. The coefficients a_1 and a_2 would be determined from the matching boundary conditions at the interface. The wave solution in the stable layer is more complicated. It depends on the stratification structure of $N^2(z)$. In the following, we discuss the wave solutions of two different stratification structures: constant stratification and continuously varying stratification. Before the discussion, we introduce the vertical component of the averaged internal wave energy flux (see Appendix B for the derivation)

$$\langle F \rangle = \frac{C \text{Im}(\psi_z/\psi)}{2k^2\sigma} |\psi|^2 , \quad (2.21)$$

where the bracket $\langle \rangle$ represents that the average is taken in a wave period, and the oper-

ator Re and Im denote the real and imaginary parts of a complex number, respectively. Given the averaged kinetic energies fluxes of the incident wave $\langle F_i \rangle$, the reflective wave $\langle F_r \rangle$, and the transmitted wave $\langle F_t \rangle$, we define the reflection ratio

$$\zeta = \frac{|\langle F_r \rangle|}{|\langle F_i \rangle|}, \quad (2.22)$$

and the transmission ratio

$$\eta = \frac{|\langle F_t \rangle|}{|\langle F_i \rangle|}. \quad (2.23)$$

Note that here the definitions of the reflection ratio and the transmission ratio are calculated by energy flux (Wei (2020) used kinetic energy but in his erratum he used energy flux). In the followings, we discuss the wave solutions in the two different stratifications.

2.1. Constant stratification in the stable layer

The case of constant stratification has been discussed in Wei (2020). Here we discuss it again in a general form for the convenience of comparison. For a constant stratification $N_{max}^2 = \gamma_1$ ($\gamma_1 > 0$), the wave solution can be written as

$$\psi = b_1 \exp(isz) + b_2 \exp(-isz), \quad (2.24)$$

where $s > 0$ and $s^2 = k^2(B^2 - A_0 C - \gamma_1 C)/C^2$ is the square of wavenumber in the vertical direction, and $s > 0$. The wave solution contains two separated branches with opposite vertical propagating directions. The selection of wave directions depends on the configurations. We consider configurations 1 and 2 in the followings, respectively.

2.1.1. Configuration 1

The vertical component of the group velocity (c_g) of the transmitted wave should be in the same direction with that of the incident wave. For configuration 1, c_g of the transmitted wave is outward. The direction of c_g is determined by the sign of C . Here we discuss the two cases $C > 0$ and $C < 0$, separately.

For the case $C > 0$ (or $\sigma^2 < f^2$), it requires $b_2 = 0$. The wave with wavenumber $+q$ is incident wave, the wave with wavenumber $-q$ is reflective wave, and the wave with wavenumber $+s$ is transmitted wave. The matching boundary conditions at the interface gives

$$a_1 + a_2 = b_1, \quad (2.25)$$

$$qa_1 - qa_2 = sb_1. \quad (2.26)$$

Note that the terms containing δ can be cancelled on both sides in the second matching boundary condition. Solving these equations, we obtain the wave amplitude ratios

$$\frac{a_2}{a_1} = \frac{q - s}{q + s}, \quad (2.27)$$

$$\frac{b_1}{a_1} = \frac{2q}{q + s}. \quad (2.28)$$

With the amplitude ratios, the reflection ratio can be calculated as

$$\zeta = \left(\frac{a_2}{a_1}\right)^2 = \left(\frac{q - s}{q + s}\right)^2, \quad (2.29)$$

and the transmission ratio can be calculated as

$$\eta = \frac{s}{q} \left(\frac{b_1}{a_1}\right)^2 = \frac{4sq}{(q + s)^2}. \quad (2.30)$$

It can be seen that

$$\zeta + \eta = 1 , \quad (2.31)$$

which means that the incident wave energy is either reflected or transmitted. We are interested in whether waves could penetrate across the interface efficiently. The efficiency can be estimated by the transmission ratio (or the reflection ratio). The higher transmission ratio (or the lower reflection ratio), the more wave energy is transmitted.

Noting $q = k\sqrt{\Delta_0}/C$ and $s = k\sqrt{\Delta_m}/C$, we can rewrite the transmission ratio as

$$\eta = 1 - \left(\frac{\sqrt{\Delta_0} - \sqrt{\Delta_m}}{\sqrt{\Delta_0} + \sqrt{\Delta_m}} \right)^2 = 1 - \left(1 - \frac{2}{\sqrt{\Delta_0/\Delta_m} + 1} \right)^2 , \quad (2.32)$$

where $\Delta_0 = B^2 - A_0C$ and $\Delta_m = B^2 - A_0C - N_{max}^2$. It can be seen that η decreases with Δ_0/Δ_m . By taking the first derivatives, it is easy to prove that Δ_0/Δ_m increases with $N_{max}^2/(2\Omega)^2$, and decreases with σ^2 . As a result, we find that η decreases with $N_{max}^2/(2\Omega)^2$ and increases with σ^2 . Specifically, we have $\eta \rightarrow 1$ when $N_{max}^2/(2\Omega)^2 \rightarrow 0$ or $\sigma^2 \rightarrow f^2$. Therefore, the transmission is efficient when the rotation is fast, or when the absolute value of the frequency is close to the vertical Coriolis parameter.

For the case $C < 0$ (or $\sigma^2 > f^2$), it requires $b_1 = 0$. The wave with wavenumber $-q$ is incident wave, the wave with wavenumber $+q$ is reflective wave, and the wave with wavenumber $-s$ is the transmitted wave. Then the boundary conditions give

$$a_1 + a_2 = b_2 , \quad (2.33)$$

$$qa_1 - qa_2 = -sb_2 . \quad (2.34)$$

Thus we have

$$\frac{a_1}{a_2} = \frac{q - s}{q + s} , \quad (2.35)$$

$$\frac{b_2}{a_2} = \frac{2q}{q + s} . \quad (2.36)$$

Now the reflection ratio is

$$\zeta = \left(\frac{a_1}{a_2} \right)^2 = \left(\frac{q - s}{q + s} \right)^2 , \quad (2.37)$$

and the transmission ratio is

$$\eta = \frac{s}{q} \left(\frac{b_2}{a_2} \right)^2 = \frac{4qs}{(q + s)^2} = 1 - \zeta . \quad (2.38)$$

Similarly, we can rewrite the transmission ratio as

$$\eta = 1 - \left(\frac{\sqrt{\Delta_0} - \sqrt{\Delta_m}}{\sqrt{\Delta_0} + \sqrt{\Delta_m}} \right)^2 = 1 - \left(1 - \frac{2}{\sqrt{\Delta_0/\Delta_m} + 1} \right)^2 . \quad (2.39)$$

Noting $\Delta_0/\Delta_m < 1$, we see that η increases with Δ_0/Δ_m . By taking derivatives, we find that Δ_0/Δ_m decreases with N_{max}^2 and σ^2 . As a result, we find that η decreases with $N_{max}^2/(2\Omega)^2$ and σ^2 . Specifically, we have $\eta \rightarrow 1$ when $N_{max}^2/(2\Omega)^2 \rightarrow 0$ or $\sigma^2 \rightarrow f^2$. Again, we conclude that the transmission ratio is efficient when the stable layer is weakly stratified, or when the wave is near the critical colatitude.

For the configuration 1, we have plotted the transmission ratios for different $N_{max}^2/(2\Omega)^2$ and $\sin^2 \alpha$ in fig. 3. The effect of $N_{max}^2/(2\Omega)^2$ is shown from the top to bottom ($N_{max}^2/(2\Omega)^2 = 10, 1, 0.1$), and the effect of $\sin^2 \alpha$ is shown from the left to right ($\sin^2 \alpha = 0.01, 0.5, 1.0$). First, we observe that the degree of stratification

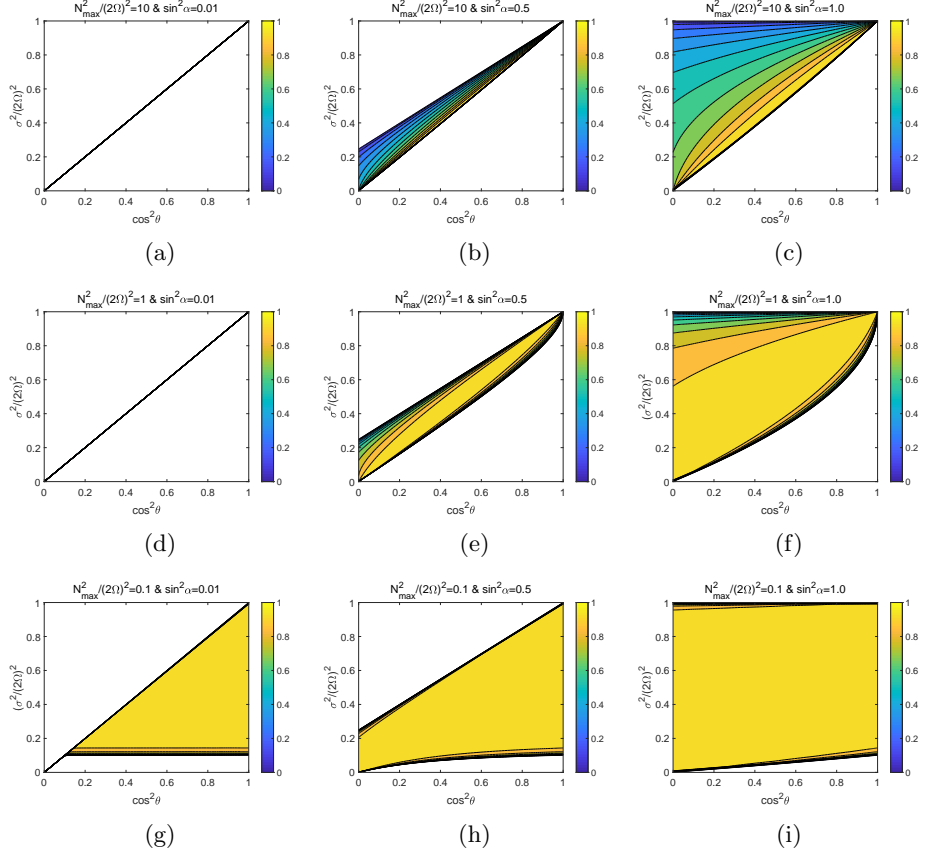


Figure 3: Transmission ratios for different $N_{max}^2/(2\Omega)^2$ and $\sin^2 \alpha$. The horizontal axis is $\cos^2 \theta$, and the vertical axis is $\sigma^2/(2\Omega)^2$. (a)-(c) The slowly rotating group ($N_{max}^2/(2\Omega)^2 = 10$) with $\sin^2 \alpha \in \{0.01, 0.5, 1.0\}$ from the left to right. (d)-(f) The moderately rotating group ($N_{max}^2/(2\Omega)^2 = 1$) with $\sin^2 \alpha \in \{0.01, 0.5, 1.0\}$ from the left to right. (g)-(i) The rapidly rotating group ($N_{max}^2/(2\Omega)^2 = 0.1$) with $\sin^2 \alpha \in \{0.01, 0.5, 1.0\}$ from the left to right.

$(N_{max}^2/(2\Omega)^2)$ has great impact on the frequency domain. The frequency domain is much wider at low (high) latitudes when the stable layer is strongly (weakly) stratified. Second, we notice that the wavenumber also has important effect on the frequency domain. The frequency domain is much wider when the meridional wavenumber dominates the zonal wavenumber. These two points have already been confirmed previously in the frequency domain analysis. Third, we notice that the transmission ratio largely depends on the degree of stratification and wave frequency. High transmission ratios are achieved when the $N_{max}^2/(2\Omega^2)$ is small (the stable layer is weakly stratified), or when $\sigma^2 - f^2 \simeq 0$ (the wave is near the critical colatitude). This result is consistent with our theoretical analysis.

2.1.2. Configuration 2

For configuration 2, the wave propagates from the stable layer to the convective layer. We discuss it in two cases $C > 0$ and $C < 0$, respectively. For the first case $C > 0$, it requires $a_1 = 0$. The waves with wavenumber $-s$, $+s$, and $-q$ are the incident wave, reflective wave, and transmitted wave, respectively. From the boundary conditions, we

obtain

$$b_1 + b_2 = a_2 , \quad (2.40)$$

$$sb_1 - sb_2 = -qa_2 . \quad (2.41)$$

The solution is

$$\frac{b_1}{b_2} = \frac{s-q}{s+q} , \quad (2.42)$$

$$\frac{a_2}{b_2} = \frac{2s}{s+q} . \quad (2.43)$$

The reflection ratio is

$$\zeta = \left(\frac{b_1}{b_2} \right)^2 = \left(\frac{s-q}{s+q} \right)^2 . \quad (2.44)$$

and the transmission ratio is

$$\eta = \frac{q}{s} \left(\frac{a_2}{b_2} \right)^2 = \frac{4sq}{(s+q)^2} = 1 - \zeta . \quad (2.45)$$

Therefore, the transmission ratio can be written as

$$\eta = 1 - \left(\frac{\sqrt{\Delta_m} - \sqrt{\Delta_0}}{\sqrt{\Delta_m} + \sqrt{\Delta_0}} \right)^2 \quad (2.46)$$

The analysis is similar to configuration 1. It is found that the transmission is efficient when the stable layer is weakly stratified, or when the wave is near the critical colatitude.

For the case $C < 0$, it requires $a_2 = 0$. The waves with wavenumber $+s$, $-s$, and $+q$ are the incident wave, reflective wave, and transmitted wave, respectively. Thus we have

$$b_1 + b_2 = a_1 , \quad (2.47)$$

$$sb_1 - sb_2 = qa_1 . \quad (2.48)$$

The solution is

$$\frac{b_2}{b_1} = \frac{s-q}{s+q} , \quad (2.49)$$

$$\frac{a_1}{b_1} = \frac{2s}{s+q} . \quad (2.50)$$

The reflection ratio is

$$\zeta = \left(\frac{b_2}{b_1} \right)^2 = \left(\frac{s-q}{s+q} \right)^2 . \quad (2.51)$$

and the transmission ratio is

$$\eta = \frac{q}{s} \left(\frac{a_1}{b_1} \right)^2 = \frac{4sq}{(s+q)^2} = 1 - \zeta . \quad (2.52)$$

Therefore, the transmission ratio can be written as

$$\eta = 1 - \left(\frac{\sqrt{\Delta_m} - \sqrt{\Delta_0}}{\sqrt{\Delta_m} + \sqrt{\Delta_0}} \right)^2 \quad (2.53)$$

The discussion is similar to configuration 1. It is found that the transmission is efficient when the stable layer is weakly stratified, or when the wave is near the critical latitude.

2.2. Continuously varying stratification in the stable layer

For a continuously varying stratification in the stable layer, we assume that $N^2(z)$ is a function of z in the region $z \in (0, z_m)$. For the existence of wave solution, it requires $B^2 - A_0 C - N^2(z)C > 0$ for $z \in (0, z_m)$. It also requires $N^2(0) = 0$ because $N^2(z)$ is assumed to be continuous at the interface. In the stable layer, we write equation (2.13) as

$$\psi_{zz} + s^2\psi = 0 , \quad (2.54)$$

where $s^2 = k^2[(B^2 - A_0 C - N^2 C)/C^2]$ and s is a function of z . We perform WKB analysis to solve this equation. Assuming $\psi \propto e^{iX(z)}$ and substituting it into the above equation, we obtain

$$iX_{zz} - X_z^2 + s^2 = 0 , \quad (2.55)$$

where $X(z)$ is assumed to be a slowly varying function. For a slowly varying function, X_{zz} is small compared to X_z^2 . Neglecting X_{zz} gives the first approximation

$$-X_z^2 + s^2 = 0 . \quad (2.56)$$

The solution is

$$X = \pm \int_0^z s(z') dz' . \quad (2.57)$$

Substituting (2.57) into (2.55), we obtain

$$X_z^2 = \pm is_z + s^2 . \quad (2.58)$$

For a slowly varying function, s_z is small compared with s . It gives the second approximation

$$X_z = \pm(\pm is_z + s^2)^{1/2} \approx \pm s + is_z/(2s) , \quad (2.59)$$

and we obtain

$$X = \frac{i}{2}[\ln s(z) - \ln s(0)] \pm \int_0^z s(z') dz' . \quad (2.60)$$

Substituting X back into ψ , we have

$$\psi \propto [s(0)/s(z)]^{1/2} e^{\pm i \int_0^z s(z') dz'} . \quad (2.61)$$

Now we assume that the general solution of ψ is

$$\psi = [s(0)/s(z)]^{1/2} \left[b_1 e^{i \int_0^z s(z') dz'} + b_2 e^{-i \int_0^z s(z') dz'} \right] . \quad (2.62)$$

Its derivative is

$$\psi_z = -2^{-1} s_z(z) s(z)^{-1} \psi + i[s(z) s(0)]^{1/2} \left[b_1 e^{i \int_0^z s(z') dz'} - b_2 e^{-i \int_0^z s(z') dz'} \right] . \quad (2.63)$$

At $z = 0$, we have

$$\psi(0) = b_1 + b_2 , \quad (2.64)$$

$$\psi_z(0) = -2q\beta\psi(0) + iq(b_1 - b_2) , \quad (2.65)$$

where $\beta = (2q)^{-2} s_z(0)$ and $s(0) = q$ have been used. Now we discuss the wave reflection and transmission for the two configurations.

2.2.1. Configuration 1

For $C > 0$, the outward transmitted wave requires $b_2 = 0$. Matching the boundary conditions at the interface, we have

$$a_1 + a_2 = b_1 , \quad (2.66)$$

$$a_1 - a_2 = 2\beta i b_1 + b_1 . \quad (2.67)$$

The solution is

$$\frac{a_2}{a_1} = \frac{-\beta i}{1 + \beta i} , \quad (2.68)$$

$$\frac{b_1}{a_1} = \frac{1}{1 + \beta i} . \quad (2.69)$$

Thus the reflection ratio at the interface is

$$\zeta = \frac{|a_2|^2}{|a_1|^2} = \frac{\beta^2}{1 + \beta^2} . \quad (2.70)$$

and the transmission ratio at the interface is

$$\eta = \frac{q |b_2|^2}{q |a_1|^2} = \frac{1}{1 + \beta^2} = 1 - \zeta . \quad (2.71)$$

The explicit form of $|\beta|$ is

$$|\beta| = \frac{|dN^2(0)/dz|C^2}{8k(B^2 - A_0C)^{3/2}} . \quad (2.72)$$

If $|\beta| \rightarrow \infty$, then $\eta \rightarrow 0$ and the incident wave is totally reflected. If $|\beta| \rightarrow 0$, then $\eta \rightarrow 1$ and the incident wave is totally transmitted. If $\infty > |\beta| > 0$, then $1 > \eta > 0$ and the incident wave is partially reflected. Let us further assume that N^2 varies as a polynomial function $N^2 = \gamma_2 z^\nu$, where $\gamma_2 > 0$ and $\nu > 0$ are constants. Making a substitution, we obtain

$$|\beta| = \frac{\gamma_2 \nu z^{\nu-1} C^2}{8k(B^2 - A_0C)^{3/2}}|_{z=0} . \quad (2.73)$$

From the above equation, we have the following conclusions:

(1) When $\nu < 1$, we have $|\beta| \rightarrow \infty$, thus the incident wave is totally reflected at the interface.

(2) When $\nu > 1$, we have $|\beta| = 0$, thus the incident wave is totally transmitted at the interface.

(3) When $\nu = 1$, we have $\infty > |\beta| > 0$, thus the incident wave is partially transmitted at the interface.

Let us now consider the special case $\nu = 1$. For this case, we have

$$|\beta| = \frac{\gamma_2 C^2}{8k(B^2 - A_0C)^{3/2}} \quad (2.74)$$

$$= \frac{N_{max}^2 C^2}{8z_m k(B^2 - A_0C)^{3/2}} \quad (2.75)$$

where the relation $N_{max}^2 = \gamma_2 z_m$ has been applied. It can be seen that $|\beta|$ decreases with $z_m k$ and increases with $N_{max}^2/(2\Omega)^2$. Also, it can be proved that $|\beta|$ decreases with σ^2 by taking derivatives. As a result, η increases with $z_m k$ and σ^2 , and decreases with $N_{max}^2/(2\Omega)^2$. Specifically, we have $\eta \rightarrow 1$ when $N_{max}^2/(2\Omega)^2 \rightarrow 0$, or $\sigma^2 \rightarrow f^2$, or

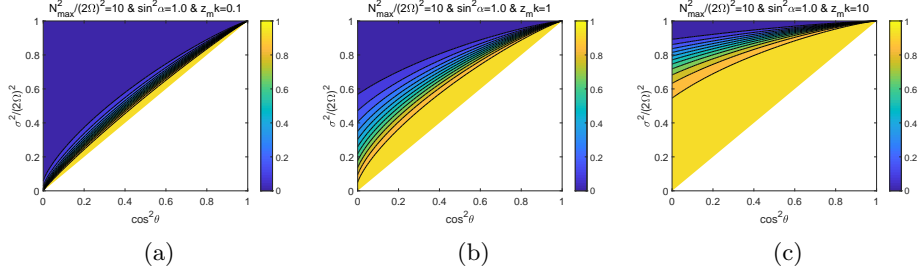


Figure 4: Transmission ratios at different $z_m k$ ($=0.1, 1, 10$ from the left to right). $N_{max}^2 = 10$ and $\sin^2 \alpha = 1.0$ for all the cases.

$z_m \gg k^{-1}$. Therefore, the transmission ratio is efficient when the stable layer is weakly stratified, or when the wave is near the critical latitude, or when the width of the linear stratification layer is far greater than the horizontal wavelength. Fig.4 illustrates the transmission contours at different $z_m k$ in a slowly rotating fluid. It clearly shows that the transmission ratio increases with $z_m k$ even when the stable layer is strongly stratified. A small value of $z_m k$ can be easily realized for short waves. It indicates that short wave is more likely to transmit in a strongly stratified fluid when the stable layer is linear stratified.

For $C > 0$, the outward transmitted wave requires $b_1 = 0$. Matching the boundary conditions at the interface, we have

$$a_1 + a_2 = b_2 , \quad (2.76)$$

$$a_1 - a_2 = 2\beta i b_2 - b_2 . \quad (2.77)$$

The solution is

$$\frac{a_1}{a_2} = \frac{\beta i}{1 - \beta i} , \quad (2.78)$$

$$\frac{b_2}{a_2} = \frac{1}{1 - \beta i} . \quad (2.79)$$

Thus the transmission ratio at the interface is

$$\eta = \frac{q |b_2|^2}{q |a_2|^2} = \frac{1}{1 + \beta^2} . \quad (2.80)$$

We see that the η has the same form with the case $C > 0$. Therefore the conclusion remains unchanged.

2.2.2. Configuration 2

For $C > 0$, the inward transmitted wave requires $a_1 = 0$. Therefore, at the interface we have

$$b_1 + b_2 = a_2 , \quad (2.81)$$

$$2i\beta(b_1 + b_2) + (b_1 - b_2) = -a_2 . \quad (2.82)$$

The solution is

$$\frac{b_1}{b_2} = \frac{-i\beta}{1 + i\beta} , \quad (2.83)$$

$$\frac{a_2}{b_2} = \frac{1}{1 + i\beta} . \quad (2.84)$$

Thus the transmission ratio is

$$\eta = \frac{q |a_2|^2}{q |b_2|^2} = \frac{1}{1 + \beta^2}. \quad (2.85)$$

The transmission ratio has the same form as configuration 1, which yields similar conclusion.

For $C < 0$, the inward transmitted wave requires $a_2 = 0$. Therefore at the interface we have

$$b_1 + b_2 = a_1, \quad (2.86)$$

$$2i\beta(b_1 + b_2) + (b_1 - b_2) = a_1. \quad (2.87)$$

The solution is

$$\frac{b_2}{b_1} = \frac{i\beta}{1 - i\beta}, \quad (2.88)$$

$$\frac{a_1}{b_1} = \frac{1}{1 - i\beta}. \quad (2.89)$$

Thus the transmission ratio is

$$\eta = \frac{q |a_1|^2}{q |b_1|^2} = \frac{1}{1 + \beta^2}. \quad (2.90)$$

The transmission ratio has the same form as configuration 1, and the conclusion remains unchanged.

3. Conclusion and Discussion

We have discussed the wave propagation in a partially stratified rotating fluid with two configurations. In configuration 1, the wave propagates from the convective layer to the stable layer. In configuration 2, the wave propagates from the stable layer to the convective layer. First, we have discussed the width of the frequency range on the existence of wave solution. We have the following major findings:

(1) When the stable layer is strongly stratified (slow rotation), waves prefer to survive at low latitudes rather than high latitudes.

(2) When the stable layer is weakly stratified (rapid rotation), waves can survive in the full sphere if the meridional wavenumber is large.

Second, we have investigated the efficiency of wave transmission in these configurations. We have not observed significant difference on the efficiency of wave transmission between these two configurations. We have considered different stratification structures in the stable layer: the constant stratification, and the continuously varying stratification. For the continuously varying stratification, we have discussed the transmission ratio when the square of buoyancy frequency N^2 varies as a polynomial function $N^2 \propto z^\nu$. We have the following major findings:

(3) For the constant stratification, the transmission at the interface is efficient when the stable layer is weakly stratified (rapid rotation), or when the wave is at the critical latitude.

(4) For the linear stratification ($\nu = 1$), the transmission at the interface is efficient when the stable layer is weakly stratified (rapid rotation), or when the wave is at the critical latitude, or when the width of the linear stratification layer is far greater than the horizontal wavelength.

(5) For a convex stratification ($\nu > 1$), there is no reflection at the interface and all of the incident wave is transmitted.

(6) For a concave stratification ($0 < \nu < 1$), there is no transmission at the interface and all of the incident wave is reflected.

For each stratification structure, it is also interesting to note that the wave transmission ratio at the interface is identical for both configurations, no matter what direction the wave propagates. It only depends on the characteristics of the wave (wave frequency and wavenumber) and the fluid (degree of stratification).

Our findings have useful applications in the prediction of wave transmission in rotating stars or planets. For example, g-mode has not been detected on the solar surface so far. Our calculation shows that the efficiency of wave transmission largely depends on the stratification structure. Waves are easy to transmit when the transition at the interface between the convective and stable layers is smooth (convex stratification is continuous but not smooth at the interface). If the transition near the base of solar convection zone is smooth, then the gravito-inertial wave excited in the stable layer can be easily transmitted into the convective layer. Then the chance of g-mode detection at the solar surface would be higher. In reality, the transition of the square of buoyancy frequency is likely to be linear below the solar convection zone (see figure 2 in Rogers & Glatzmaier (2005)). The rotation speed of the Sun is slow, and the stable layer is strongly stratified. For this case, gravity waves are more likely to transmit at low latitudes, when the wave is at the critical latitude, or when its horizontal wavelength is small. Thus the chance on the detection of solar g-mode would be higher for short waves at low latitudes. The amplitude of short wave is usually small, because wave amplitude usually decreases with wavenumber and frequency. Therefore, the detection of solar g-mode would be difficult. Our result also shows that wave propagation might be important in rapidly rotating stars. For example, material mixing near the core boundary has important effect on the evolution of low- and intermediate-mass stars (Claret & Torres 2019). For rapidly rotating low- and intermediate-mass stars, inertial waves excited in the convective core region could transmit efficiently into the upper stable layer as gravito-inertial waves. Momentum and energy could possibly be transported spontaneously, which might facilitate the material mixing near the core boundary. Our analysis is based on f -plane in Cartesian coordinates. Linear instability analysis of rotating viscous flow has shown that teleconvection (fluid motion is vigorous in the stable layer) can be driven when the stable layer is weakly stratified in spherical geometry (Zhang & Schubert 2002). This phenomenon has also been verified in the analysis of rapidly rotating viscous flow in f -planes (Cai 2020). These results have borne some similarities with our conclusions. So probably our arguments still hold in other geometries. It would be interesting to verify them in different geometries.

T.C. has been supported by NSFC (No.11503097), the Guangdong Basic and Applied Basic Research Foundation (No.2019A1515011625), the Science and Technology Program of Guangzhou (No.201707010006), the Science and Technology Development Fund, Macau SAR (Nos.0045/2018/AFJ, 0156/2019/A3), and the China Space Agency Project (No.D020303). C.Y. has been supported by the National Natural Science Foundation of China (grants 11373064, 11521303, 11733010, 11873103), Yun-nan National Science Foundation (grant 2014HB048), and Yunnan Province (2017HC018). X.W. has been supported by National Natural Science Foundation of China (grant no.11872246) and Beijing Natural Science Foundation (grant no. 1202015). This work is partially supported by Open Projects Funding of Lunar and Planetary Science Laboratory, MUST — Partner Laboratory of Key Laboratory of Lunar and Deep Space

Exploration, CAS (Macau FDCT grant No. 119/2017/A3).

Declaration of Interests. The authors report no conflict of interest.

Author ORCID. T. Cai, <https://orcid.org/0000-0003-3431-8570>; Y. Cong, <https://orcid.org/0000-0003-0454-7890>; X. Wei, <https://orcid.org/0000-0002-8033-2974>

Appendix A.

The width of the frequency range is

$$\sigma_{max}^2 - \sigma_{min}^2 = \frac{1}{2}[(f^2 + \tilde{f}_s^2 - N_{max}^2) + \sqrt{(f^2 + \tilde{f}_s^2 - N_{max}^2)^2 + 4N_{max}^2 \tilde{f}_s^2}] . \quad (\text{A } 1)$$

Here we investigate the monotonicity of $\sigma_{max}^2 - \sigma_{min}^2$ on θ . It is equivalent to consider the monotonicity of the following function

$$G(\theta, \mu_1, \mu_2) = G_1(\theta, \mu_1, \mu_2) + \sqrt{G_1^2(\theta, \mu_1, \mu_2) + 4G_2(\theta, \mu_1, \mu_2)} , \quad (\text{A } 2)$$

where $G_1(\theta, \mu_1, \mu_2) = \cos^2 \theta + \mu_1 \sin^2 \theta - \mu_2$, $G_2(\theta, \mu_1, \mu_2) = \mu_1 \mu_2 \sin^2 \theta$, $\mu_1 = \sin^2 \alpha$, and $\mu_2 = N_{max}^2 / (2\Omega)^2$. Taking the first derivative on θ , we have

$$G_\theta = G_{1\theta} + \frac{G_1 G_{1\theta} + 2G_{2\theta}}{\sqrt{G_1^2 + 4G_2}} , \quad (\text{A } 3)$$

Setting $G_\theta(\theta) = 0$, we obtain

$$G_{1\theta}^2(G_1^2 + 4G_2) = (G_1 G_{1\theta} + 2G_{2\theta})^2 , \quad (\text{A } 4)$$

or in another form

$$G_{1\theta}^2 G_2 = G_1 G_{1\theta} G_{2\theta} + G_{2\theta}^2 . \quad (\text{A } 5)$$

From the above equation, we obtain that the critical point should satisfy

$$\mu_2 = 1 - \mu_1 \quad (\text{A } 6)$$

Therefore, $G_\theta > 0$ when $\mu_2 > 1 - \mu_1$, and $G_\theta < 0$ when $\mu_2 < 1 - \mu_1$. It can be easily found that $1 - \mu_1$ is within the range $[0, 1]$. Thus we have the following conclusion. If $\mu_2 > 1$, then $\sigma_{max}^2 - \sigma_{min}^2$ increases with θ . If $\mu_2 < 1$, there exists a critical value $\mu_{1c} = 1 - \mu_2$, and $\sigma_{max}^2 - \sigma_{min}^2$ increases (decreases) with θ when $\mu_1 > \mu_{1c}$ ($\mu_1 < \mu_{1c}$). Fig.5(a) and (b) presents two cases with $\mu_2 < 1$ and $\mu_2 > 1$, respectively. Fig.5(b) clearly shows that $G(\theta)$ increases with θ when $\mu_2 > 1$. Fig.5(a) shows that the trend of $G(\theta)$ depends on a critical value μ_{1c} when $\mu_2 < 1$.

Taking the first derivative on μ_1 , we have

$$G_{\mu_1} = G_{1\mu_1} + \frac{G_1 G_{1\mu_1} + 2G_{2\mu_1}}{\sqrt{G_1^2 + 4G_2}} \quad (\text{A } 7)$$

$$= (1 + \frac{\cos^2 \theta + \mu_1 \sin^2 \theta + \mu_2}{\sqrt{G_1^2 + 4G_2}}) \sin^2 \theta \quad (\text{A } 8)$$

$$\geq 0 \quad (\text{A } 9)$$

Therefore, $\sigma_{max}^2 - \sigma_{min}^2$ increases with μ_1 .

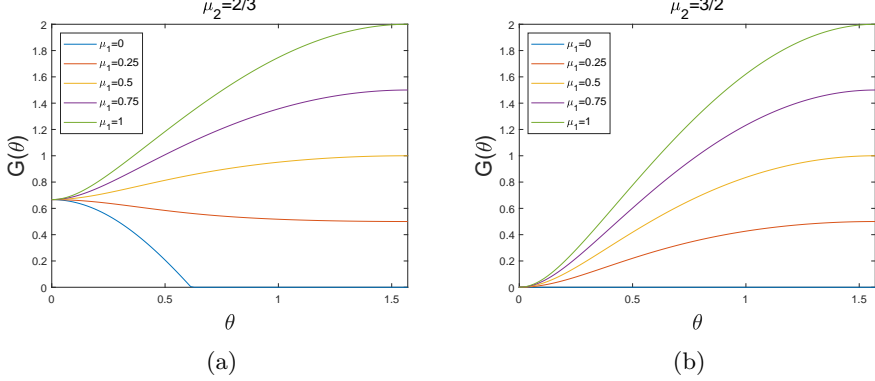


Figure 5: (a) $G(\theta)$ as a function of θ when $\mu_2 = 2/3$. In this case, $\mu_2 < 1$ and $\mu_{1c} = 1/3$. (b) $G(\theta)$ as a function of θ when $\mu_2 = 3/2$. In this case, $\mu_2 > 1$.

Taking the first derivative on μ_2 , we have

$$G_{\mu_2} = G_{1\mu_2} + \frac{G_1 G_{1\mu_2} + 2G_{2\mu_2}}{\sqrt{G_1^2 + 4G_2}} \quad (\text{A 10})$$

$$= \frac{\mu_1 \sin^2 \theta + \mu_2 - \cos^2 \theta - \sqrt{G_1^2 + 4G_2}}{\sqrt{G_1^2 + 4G_2}} \quad (\text{A 11})$$

$$= \frac{-4\mu_1 \sin^2 \theta \cos^2 \theta}{(\sqrt{G_1^2 + 4G_2})(\mu_1 \sin^2 \theta + \mu_2 - \cos^2 \theta + \sqrt{G_1^2 + 4G_2})} \quad (\text{A 12})$$

$$\leq 0 \quad (\text{A 13})$$

Therefore, $\sigma_{max}^2 - \sigma_{min}^2$ decreases with μ_2 .

Appendix B.

Applying the operation $\nabla \times$ to (2.2), we obtain the vorticity equation

$$(\nabla \times \mathbf{u})_t + \nabla \times (\mathbf{f} \times \mathbf{u}) - \nabla b \times \hat{z} = 0. \quad (\text{B 1})$$

From this equation, we can obtain the vertical component of vorticity

$$\hat{z} \cdot \nabla \times \mathbf{u} = -\frac{1}{i\sigma} (\mathbf{f} \cdot \nabla) w. \quad (\text{B 2})$$

It can be rearranged as

$$u \sin \alpha - v \cos \alpha = -\frac{1}{\sigma k} (f w_z + i k \tilde{f}_s w). \quad (\text{B 3})$$

From the continuity equation (2.3), we have

$$u \cos \alpha + v \sin \alpha = \frac{i}{k} w_z \quad (\text{B 4})$$

Solving (B 3) and (B 4), we get the horizontal velocities

$$u = \frac{(i\sigma \cos \alpha - f \sin \alpha) w_z - (i k \tilde{f}_s \sin \alpha) w}{k \sigma}, \quad (\text{B 5})$$

$$v = \frac{(i\sigma \sin \alpha + f \cos \alpha) w_z + (i k \tilde{f}_s \cos \alpha) w}{k \sigma}. \quad (\text{B 6})$$

Now we consider the energy equation. Applying the operator $\mathbf{u} \cdot$ to (2.2), we obtain the kinetic energy conservation equation

$$\left(\frac{1}{2}|\mathbf{u}|^2\right)_t + \mathbf{u} \cdot \nabla p - bw = 0 , \quad (\text{B } 7)$$

where $E_{kin} = |\mathbf{u}|^2/2$ is the kinetic energy. Multiplying (2.3) with b/N^2 , we obtain the potential energy conservation equation

$$\left(\frac{b^2}{2N^2}\right)_t + bw = 0 , \quad (\text{B } 8)$$

where $E_{pe} = b^2/(2N^2)$ is the potential energy. Adding (B 7) and (B 8), we have

$$\left(\frac{|\mathbf{u}|^2}{2} + \frac{b^2}{2N^2}\right)_t + \nabla \cdot (p\mathbf{u}) = 0 , \quad (\text{B } 9)$$

where $E_{wave} = (|\mathbf{u}|^2 + b^2/N^2)/2$ is the wave energy. With the explicit forms of horizontal velocities (B 5) and (B 6), we can calculate the averaged kinetic energy

$$\begin{aligned} \langle E_{kin} \rangle &= \frac{1}{2} \langle \text{Re}(u)^2 + \text{Re}(v)^2 + \text{Re}(w)^2 \rangle \\ &= \frac{1}{4} (|u|^2 + |v|^2 + |w|^2) \\ &= \frac{1}{4\sigma^2 k^2} [|f\Psi_z/\Psi + ik\tilde{f}_s|^2 + \sigma^2(|\Psi_z/\Psi|^2 + k^2)]|\psi|^2 . \end{aligned} \quad (\text{B } 10)$$

From (2.3), the buoyancy has a form of

$$b = -\frac{1}{i\sigma} N^2 w . \quad (\text{B } 11)$$

From this equation, we can deduce the averaged potential energy

$$\langle E_{pe} \rangle = \frac{1}{2N^2} \langle \text{Re}(b)^2 \rangle = \frac{1}{4N^2} |b|^2 = \frac{N^2}{4\sigma^2} |w|^2 . \quad (\text{B } 12)$$

Therefore, the averaged wave energy can be written as

$$\begin{aligned} \langle E_{wave} \rangle &= \langle E_{kin} \rangle + \langle E_{pe} \rangle \\ &= \frac{1}{4\sigma^2 k^2} [|f\Psi_z/\Psi + ik\tilde{f}_s|^2 + \sigma^2(|\Psi_z/\Psi|^2 + k^2) + N^2 k^2]|\psi|^2 . \end{aligned} \quad (\text{B } 13)$$

Now we calculate the internal wave energy flux. The modified pressure p can be evaluated from (2.2) by

$$\begin{aligned} p &= \frac{1}{ik \sin \alpha} (i\sigma v - fu) \\ &= \frac{[(f^2 - \sigma^2)\text{Im}(w_z/w) + k\tilde{f}_s f] + i[k\tilde{f}\sigma \cos \alpha - (f^2 - \sigma^2)\Re(w_z/w)]}{k^2 \sigma} w . \end{aligned} \quad (\text{B } 14)$$

Note that the continuous of pressure perturbation (Lagrangian pressure perturbation is equal to Eulerian pressure perturbation in this case) at the interface requires that w_z is continuous. The vertical component of the averaged internal wave energy flux is

$$\begin{aligned} \langle F \rangle &= \langle \text{Re}(p)\text{Re}(w) \rangle \\ &= \left\langle \frac{[(f^2 - \sigma^2)\text{Im}(w_z/w) + k\tilde{f}_s f]\text{Re}(w)\text{Re}(w) - [k\tilde{f}\sigma \cos \alpha - (f^2 - \sigma^2)\text{Re}(w_z/w)]\text{Im}(w)\text{Re}(w)}{k^2 \sigma} \right\rangle \end{aligned}$$

$$\begin{aligned}
&= \frac{(f^2 - \sigma^2)\text{Im}(\Psi_z/\Psi) + k\tilde{f}_s f}{2k^2\sigma} |\Psi|^2 \\
&= \frac{C\delta + C\text{Im}(\psi_z/\psi) + kB}{2k^2\sigma} |\psi|^2 \\
&= \frac{C\text{Im}(\psi_z/\psi)}{2k^2\sigma} |\psi|^2.
\end{aligned} \tag{B 13}$$

REFERENCES

BOWMAN, DOMINIC M., BURSSENS, SIEMEN, PEDERSEN, MAY G., JOHNSTON, COLE, AERTS, CONNY, BUYSSCHAERT, BRAM, MICHELSSEN, MATHIAS, TKACHENKO, ANDREW, ROGERS, TAMARA M., EDELMANN, PHILIPP V. F., RATNASINGAM, RATHISH P., SIMÓN-DÍAZ, SERGIO, CASTRO, NORBERTO, MORAVVEJI, EHSAN, POPE, BENJAMIN J. S., WHITE, TIMOTHY R. & DE CAT, PETER 2019 Low-frequency gravity waves in blue supergiants revealed by high-precision space photometry. *Nature Astronomy* **3**, 760–765.

CAI, TAO 2020 Penetrative Convection for Rotating Boussinesq Flow in Tilted F-Planes. *The Astrophysical Journal, in publication*.

CLARET, ANTONIO & TORRES, GUILLERMO 2019 The Dependence of Convective Core Overshooting on Stellar Mass: Reality Check and Additional Evidence. *The Astrophysical Journal* **876** (2), 134.

FULLER, JIM, LECOANET, DANIEL, CANTIELLO, MATTEO & BROWN, BEN 2014 Angular Momentum Transport via Internal Gravity Waves in Evolving Stars. *The Astrophysical Journal* **796** (1), 17.

GERKEMA, THEO & SHRIRA, VICTOR I. 2005 Near-inertial waves in the ocean: beyond the “traditional approximation”. *Journal of Fluid Mechanics* **529**, 195–219.

GOODMAN, J. & LACKNER, C. 2009 Dynamical Tides in Rotating Planets and Stars. *The Astrophysical Journal* **696** (2), 2054–2067.

KUMAR, PAWAN, TALON, SUZANNE & ZAHN, JEAN-PAUL 1999 Angular Momentum Redistribution by Waves in the Sun. *The Astrophysical Journal* **520** (2), 859–870.

LIU, SHANG-FEI, HORI, YASUNORI, MÜLLER, SIMON, ZHENG, XIAOCHEN, HELLED, RAVIT, LIN, DOUG & ISELLA, ANDREA 2019 The formation of Jupiter’s diluted core by a giant impact. *Nature* **572** (7769), 355–357.

MATHIS, S., NEINER, C. & TRAN MINH, N. 2014 Impact of rotation on stochastic excitation of gravity and gravito-inertial waves in stars. *Astronomy & Astrophysics* **565**, A47.

OGILVIE, G. I. & LIN, D. N. C. 2004 Tidal Dissipation in Rotating Giant Planets. *The Astrophysical Journal* **610** (1), 477–509.

QU, ZHIPENG, HUANG, YI, VAILLANCOURT, PAUL A., COLE, JASON N. S., MILBRANDT, JASON A., YAU, MAN-KONG, WALKER, KALEY & DE GRANDPRÉ, JEAN 2020 Simulation of convective moistening of the extratropical lower stratosphere using a numerical weather prediction model. *Atmospheric Chemistry & Physics* **20** (4), 2143–2159.

RIEUTORD, M. 2015 *Fluid Dynamics: An Introduction*. Springer International Publishing.

RIEUTORD, M., GEORGEOT, B. & VALDETTARO, L. 2001 Inertial waves in a rotating spherical shell: attractors and asymptotic spectrum. *Journal of Fluid Mechanics* **435** (1), 103–144.

ROGERS, TAMARA M. & GLATZMAIER, GARY A. 2005 Gravity waves in the Sun. *Monthly Notices of the Royal Astronomical Society* **364** (4), 1135–1146.

ROGERS, T. M., LIN, D. N. C. & LAU, H. H. B. 2012 Internal Gravity Waves Modulate the Apparent Misalignment of Exoplanets around Hot Stars. *The Astrophysical Journal Letters* **758** (1), L6.

ROGERS, T. M., LIN, D. N. C., McELWAINE, J. N. & LAU, H. H. B. 2013 Internal Gravity Waves in Massive Stars: Angular Momentum Transport. *The Astrophysical Journal* **772** (1), 21.

ROGERS, T. M. & McELWAINE, J. N. 2017 On the Chemical Mixing Induced by Internal Gravity Waves. *The Astrophysical Journal Letters* **848** (1), L1.

WEI, XING 2020 Wave Reflection and Transmission at the Interface of Convective and Stably Stratified Regions in a Rotating Star or Planet. *The Astrophysical Journal* **890** (1), 20.

WU, YANQIN 2005a Origin of Tidal Dissipation in Jupiter. I. Properties of Inertial Modes. *The Astrophysical Journal* **635** (1), 674–687.

WU, YANQIN 2005b Origin of Tidal Dissipation in Jupiter. II. The Value of Q. *The Astrophysical Journal* **635** (1), 688–710.

YU, CONG 2020 Thermally Driven Angular Momentum Transport in Hot Jupiters. *The Astrophysical Journal Letters* **893** (1), L22.

ZAHN, J. P., TALON, S. & MATIAS, J. 1997 Angular momentum transport by internal waves in the solar interior. *Astronomy and Astrophysics* **322**, 320–328, arXiv: astro-ph/9611189.

ZHANG, KEKE & SCHUBERT, GERALD 2002 From Penetrative Convection to Teleconvection. *The Astrophysical Journal* **572** (1), 461–476.